Human Molecular Genetics, 2009, Vol. 18, No. 17 **3194–3205**
doi:10.1093/hmg/ddp257
Advance Access published on May 29, 2009

Mitochondrial abnormalities, energy deficit and oxidative stress are features of calpain 3 deficiency in skeletal muscle

Irina Kramerova[1], Elena Kudryashova[1], Benjamin Wu[1], Sean Germain[3], Krista Vandenborne[3], Nadine Romain[4], Ronald G. Haller[5,6,7], M. Anthony Verity[2] and Melissa J. Spencer[1,*]

[1]Department of Neurology and [2]Department of Pathology and Laboratory Medicine, David Geffen School of Medicine at University of California, Los Angeles, CA 90095, USA, [3]Department of Physical Therapy, University of Florida, Gainesville, FL 32610, USA, [4]Institute of Exercise and Environmental Medicine, Dallas, TX 75231, USA, [5]Department of Neurology, University of Texas Southwestern Medical School, Dallas, TX 75390, USA, [6]Institute of Exercise and Environmental Medicine, Dallas, TX 75231, USA and [7]Dallas VA Medical Center, Dallas, TX 75216, USA

Received April 30, 2009; Revised and Accepted May 27, 2009

Mutations in the non-lysosomal cysteine protease calpain-3 cause autosomal recessive limb girdle muscular dystrophy. Pathological mechanisms occurring in this disease have not yet been elucidated. Here, we report both morphological and biochemical evidence of mitochondrial abnormalities in calpain-3 knockout (C3KO) muscles, including irregular ultrastructure and distribution of mitochondria. The morphological abnormalities in C3KO muscles are associated with reduced *in vivo* mitochondrial ATP production as measured by ^{31}P magnetic resonance spectroscopy. Mitochondrial abnormalities in C3KO muscles also correlate with the presence of oxidative stress; increased protein modification by oxygen free radicals and an elevated concentration of the anti-oxidative enzyme Mn-superoxide dismutase were observed in C3KO muscles. Previously we identified a number of mitochondrial proteins involved in β-oxidation of fatty acids as potential substrates for calpain-3. In order to determine if the mitochondrial abnormalities resulted from the loss of direct regulation of mitochondrial proteins by calpain-3, we validated the potential substrates that were identified in previous proteomic studies. This analysis showed that the β-oxidation enzyme, VLCAD, is cleaved by calpain-3 *in vitro*, but we were not able to confirm that VLCAD is an *in vivo* substrate for calpain-3. However, the activity of VLCAD was decreased in C3KO mitochondrial fractions compared with wild type, a finding that likely reflects a general mitochondrial dysfunction. Taken together, these data suggest that mitochondrial abnormalities leading to oxidative stress and energy deficit are important pathological features of calpainopathy and possibly represent secondary effects of the absence of calpain-3.

INTRODUCTION

Calpain 3 (CAPN3) is a tissue-specific member of a family of non-lysosomal cysteine proteases that includes about 15 members (1,2). Mutations in CAPN3 cause an autosomal recessive form of limb girdle muscular dystrophy type 2A (LGMD2A) (3). LGMD2A is one of the most frequently occurring forms of LGMD which is characterized by a very high genetic variability (4–6). About 300 pathogenic mutations that are spread along the entire length of the gene (Leiden Muscular Dystrophy Database) have been identified. Most of these mutations are missense mutations that may or may not affect the proteolytic activity of CAPN3 (7). A comprehensive analysis of the distribution and genotype–phenotype correlation of CAPN3 mutations can be found in several studies of European populations (8,9).

Severity of LGMD2A can vary considerably even within a family. The onset of the disease is usually in the second

*To whom correspondence should be addressed at: 635 Charles Young Drive, NRB, Room 401, Los Angeles, CA 90095, USA. Tel: +1 3107945225; Fax: +1 3102061998; Email: mspencer@mednet.ucla.edu

decade of life but was reported to occur as early as 2.5 years and as late as 49 years of age. Predominant symmetrical and simultaneous involvement of pelvic and scapular girdle and trunk muscles without facial, oculo-motor or cardiac involvements is typical for LGMD2A (10,11). However, the course of disease progression as well as muscles affected by the disease can differ between LGMD2A patients. Characteristic histopathological features of LGMD2A include necrosis and regeneration, fiber diameter variability and/or atrophy (12–14). Electron microscopy examination of LGMD2A biopsies also revealed myofibrillar and mitochondrial abnormalities (12,13).

Molecular mechanisms of LGMD2A remain poorly understood. One of the difficulties in elucidating the pathological consequences of CAPN3 deficiency is that CAPN3 can potentially have a large number of substrates and binding partners and thus affect multiple cellular pathways (5). Moreover, CAPN3 deficiency could potentially have secondary effects, i.e. effects that do not derive from the direct deregulation of CAPN3 substrates. This lack of understanding of CAPN3 biological roles has made elucidation of pathogenic mechanisms, and subsequent therapies, elusive.

To study the biological role of CAPN3, several genetic models have been generated, both deficient for CAPN3 (calpain-3 knockout, C3KO) (15,16) and overexpressing full-length or alternatively spliced CAPN3 transgenes (C3Tg) (17). C3KO mice show features typical of a mild form of LGMD2A that include muscle atrophy, necrosis and regeneration and fiber diameter variability (15). Studies of C3KO mice have implicated CAPN3 in the regulation of diverse cellular processes such as apoptosis and cytoskeletal re-arrangements (15,18–22). Our studies have shown that CAPN3 is necessary for the proper control of myoblast fusion and for their transition to the terminal stages of muscle differentiation. In the absence of CAPN3, late events of myogenesis, such as sarcomere formation, were observed to be greatly inhibited. Accordingly, C3KO mice have a reduced muscle mass and decreased rate of muscle growth in response to changes in muscle loading (18,19).

Upon fractionation of skeletal muscle extracts derived from post-natal mice, CAPN3 was found in several of the fractions including the myofibrillar, cytosolic and membrane fractions (23). On the basis of these and previous studies, it is reasonable to hypothesize that CAPN3 performs different roles at each site. For example, CAPN3 is believed to be anchored to the sarcomere through its interaction with a large myofibrillar protein titin, which serves as a scaffold for sarcomeric proteins. Localization of CAPN3 in close proximity to myofibrillar proteins may allow it to play a role in their turnover (18,24,25). Recently, a novel role for membrane-associated CAPN3 was uncovered. We showed that at the skeletal muscle triad, CAPN3 acts as a structural component that anchors aldolase and ryanodine receptors and ultimately regulates calcium release (23). CAPN3 was also shown to interact with dysferlin and AHNAK and may play a role in the regulation of the dysferlin complex (26). Thus, CAPN3 has diverse cellular roles as both a protease and, possibly, a structural protein.

In order to further elucidate the biological role(s) of CAPN3, we performed a search for potential CAPN3 substrates using a proteomic approach (27). In these studies, two-dimensional gel electrophoresis was used to compare the proteomes of wild-type (WT) and C3Tg mice to identify spots that had decreased upon CAPN3 overexpression. It was presumed that proteins that showed a reduced concentration upon CAPN3 overexpression would be candidate *in vivo* substrates. As a result of these studies, a number of mitochondrial enzymes, particularly enzymes involved in β-oxidation of fatty acids, were identified as potential substrates for CAPN3 proteolytic activity (27). Since mitochondrial abnormalities were reported to be a pathological feature of LGMD2A, we investigated the status of the mitochondria in C3KO mice and used this model to address the question of whether CAPN3 directly regulates mitochondrial enzymes as was suggested by our proteomics data. In this study, we used morphological, histochemical and biochemical methods to show that, similar to LGMD2A patients, mitochondria are abnormal in C3KO muscles. These abnormalities led to decreased ATP production and increased oxidative stress in C3KO muscle. These studies identify mitochondrial dysfunction as a feature of LGMD2A and suggest that therapeutic correction of the mitochondrial abnormalities may be beneficial for the treatment of patients with this disorder.

RESULTS

Disorganized and swollen mitochondria are present in C3KO muscles

Previously, we generated CAPN3-deficient mice and characterized their phenotype. We found that these mice replicate many features of a mild form of LGMD2A, including abnormalities of muscle ultrastructure (15). We also noticed that the mitochondria were disorganized in C3KO mice. Interestingly, both electron microscopy and histochemical staining of human LGMD2A biopsies also revealed abnormalities in mitochondrial structure and distribution (12,13). In this study, we performed additional electron microscopic examination of C3KO muscles and found that not only are mitochondria disorganized in C3KO soleus (Fig. 1A–C) and diaphragm (Fig. 1D) muscles but in many cases the mitochondria had a swollen appearance with disrupted membranes (Fig. 1C, E and F).

Because of these observations of abnormal mitochondria in C3KO muscles, we further compared C3KO and WT mitochondrial distribution by histochemical methods. NADH staining (Fig. 2) confirmed an uneven distribution of mitochondria in C3KO diaphragm muscles, especially in older animals (1 year old). A similar uneven pattern was observed after SDH staining (not shown) of skeletal muscle. Thus, the presence of morphologically abnormal mitochondria is a feature of calpainopathy in both human and mouse muscle. These findings further validate the use of the C3KO mouse for the study of mitochondrial abnormalities associated with LGMD2A.

C3KO mitochondria are functionally deficient

To investigate whether structural abnormalities of mitochondria in C3KO muscles translate into functional deficits, we compared the *in vivo* mitochondrial ATP production in intact C3KO and WT gastrocnemius muscles using ^{31}P magnetic

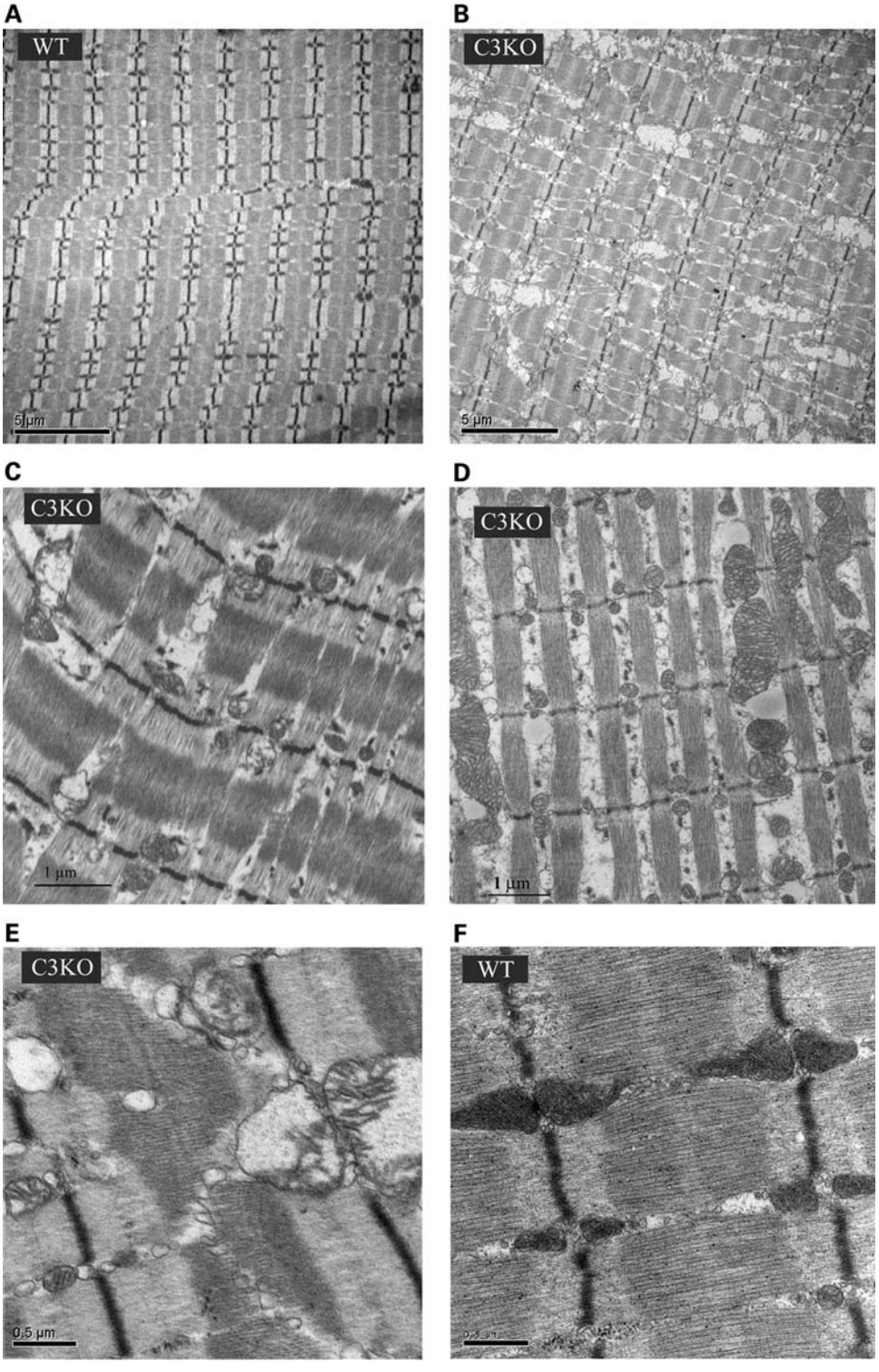

Figure 1. Ultrastructural abnormalities in mitochondria of C3KO muscles. Electron micrographs of WT soleus (**A** and **F**) and C3KO soleus muscles (**B, C** and **E**) and diaphragm (**D**) reveal disorganized mitochondria in C3KO muscles. Higher magnification images show swollen mitochondria with disrupted cristae in C3KO muscle (E).

resonance (^{31}P-MR) spectroscopy. ^{31}P-MR spectra of 6–7-month-old C3KO and WT mice collected at rest showed no significant differences in resting metabolite concentration or intracellular pH (pHi), although the phosphocreatine (PCr) concentration in the C3KO tended to be lower (25.3 ± 0.8 versus 29.2 ± 2.0 mM). As anticipated, during 30 min of ischemia, there was a gradual decrease in muscle PCr and a concomitant increase in inorganic phosphate (Pi), followed by

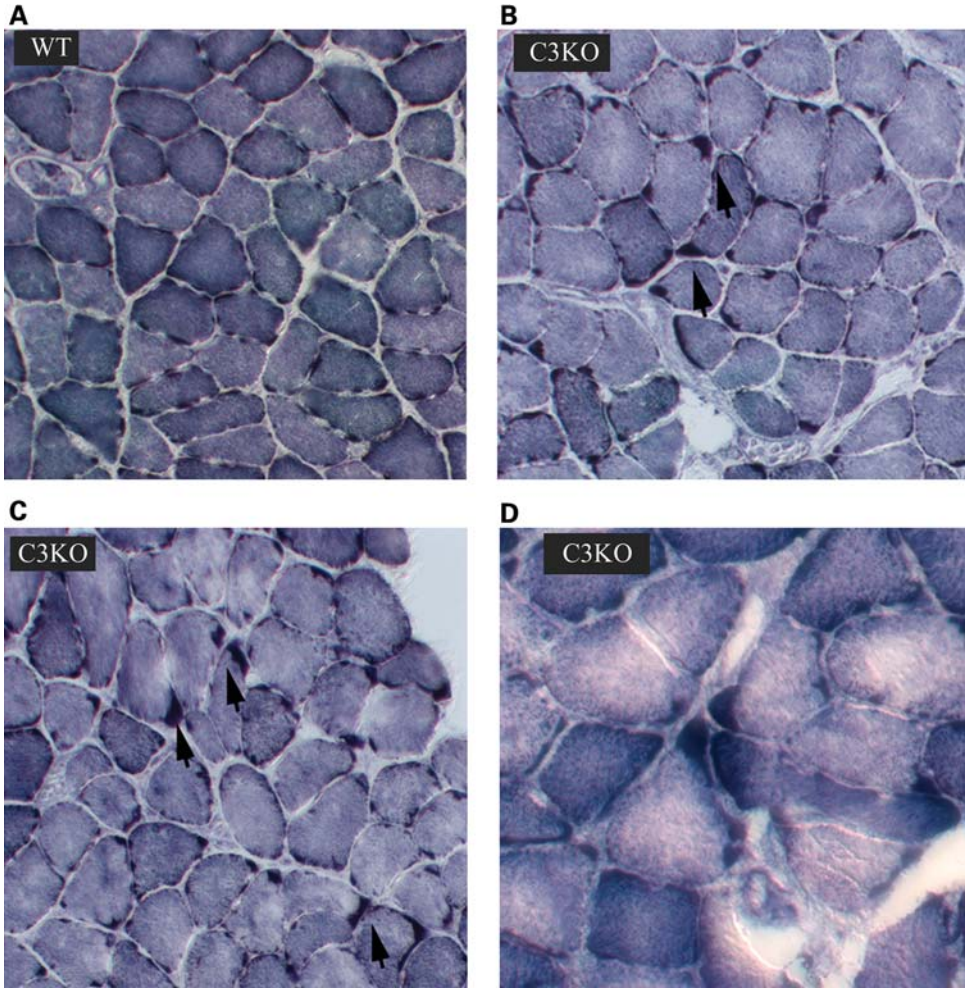

Figure 2. NADH staining of muscle sections from 1-year-old C3KO and WT mice. Staining for NADH shows an uneven distribution of mitochondria in C3KO diaphragms (**B**–**D**) compared with WT diaphragms (**A**); arrows point to the areas of mitochondrial accumulation in C3KO muscles.

a progressive recovery after the restoration of blood flow. During 30 min of ischemia, the PCr levels decreased by 45–55%, whereas Pi levels increased ~5-fold over the baseline. The pHi and ATP concentration did not change during the experiment. Despite similar pH levels at the end of ischemia, the initial rate of PCr resynthesis was significantly ($P < 0.05$) slower in the C3KO compared with WT mice. The initial rate of PCr resynthesis was 5.3 mM/min in WT mice and 3.0 mM/min in C3KO mice (Fig. 3A and B).

Decreased ATP production and energy deficit often lead to a compensatory mitochondrial proliferation. This increase in mitochondria number happens, for example, in respiratory chain disorders (28). To address the question of whether or not there is a compensatory amplification of mitochondria in C3KO muscles, we measured the biochemical activity of citrate synthase, a mitochondrial matrix enzyme which is often used as a marker of a total mitochondrial content. These experiments showed a 24% increase in citrate synthase activity in total extracts of C3KO diaphragm and 16% in total extracts of C3KO tibialis anterior muscles compared with the corresponding WT muscles (Fig. 3C), thus suggesting that mitochondrial proliferation is a feature of calpainopathy.

Evaluation of mitochondrial proteins as potential substrates of CAPN3

Although the findings of abnormal mitochondrial function in C3KO revealed a correlation between loss of CAPN3 and reduced ATP production, it is not yet clear whether these defects result from the loss of direct proteolytic regulation of mitochondrial proteins by CAPN3. Previously, we used a proteomic approach to identify potential substrates of CAPN3. Comparison of the proteomes of C3Tg mice and their non-transgenic counterparts by two-dimensional gel electrophoresis identified several metabolic enzymes, five of which are known to operate in the β-oxidation of fatty acids, suggesting that CAPN3 might be directly involved in the regulation of mitochondrial proteins by proteolytic cleavage and that the loss of this function could trigger an inability to produce ATP in the mitochondria (27).

In order to understand whether CAPN3 directly regulates mitochondrial proteins, we first determined whether previously identified enzymes of β-oxidation can be cleaved by CAPN3 *in vitro*. A schematic of the β-oxidation of fatty acids that occurs in association with the inner mitochondrial

A Rate of Pcr synthesis in individual animals, mM/min

Genotype	1	2	3	4	5	6	7	8	Average
C3KO	3.62	3.50	2.45	4.63	1.65	2.08	2.44	3.50	**2.98±0.99**
WT	4.95	4.39	5.17	7.88	6.69	6.81	3.20	n/a	**5.58±1.6**

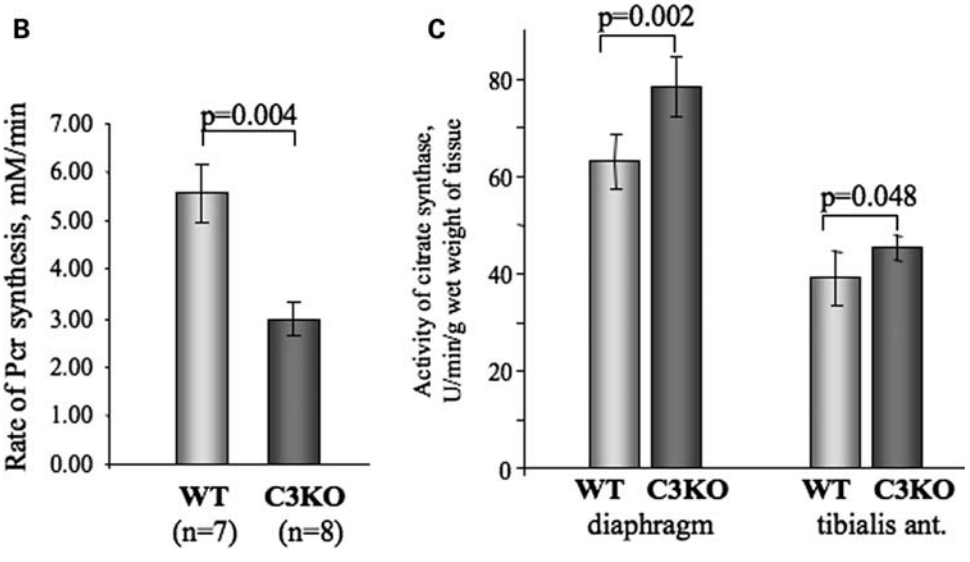

Figure 3. Rate of PCr synthesis *in vivo* is decreased in C3KO muscles. A reversible ischemia model was used to study kinetic changes in the rate of PCr synthesis *in vivo* (see Materials and Methods). (**A**) Table indicating the rate of PCr synthesis in individual mice. Initial rate of PCr synthesis was measured by ^{31}P-MR spectroscopy in eight C3KO and seven WT mice. (**B**) An average initial rate of PCr synthesis was 53.4% slower in C3KO group compared with WT group; $P < 0.05$. (**C**) Level of citrate synthase activity was increased by 24% in C3KO diaphragms and by 16% in C3KO tibialis anterior muscles compared with WT ($n = 5$ for each group).

membrane is shown in Figure 4A (proteins identified as potential CAPN3 substrates are boxed). The cDNA that codes for each of the putative substrates was isolated from muscle mRNA by RT–PCR and cloned into an insect baculovirus-based expression vector. To identify recombinant proteins, a V5 epitope was introduced at the C-terminus of each protein.

In order to validate whether CAPN3 could cleave the potential substrates, individual enzymes were co-expressed with either proteolytically active or inactive (carrying C129S mutation) forms of CAPN3. As shown in Figure 4B and C, of all potential substrates tested, only VLCAD was cleaved by CAPN3 upon co-expression in the insect cells. All other proteins that were tested demonstrated resistance to CAPN3 proteolytic activity, since no difference in concentration or molecular weight was found after co-expression with active forms of CAPN3 or inactive C129S mutant (Fig. 4C). Thus, among the five potential substrates of β-oxidation identified by initial proteomic studies, only VLCAD was cleaved by CAPN3.

VLCAD concentration *in vivo* is not regulated by CAPN3

To verify whether VLCAD is a bona fide substrate of CAPN3, we compared the concentration of VLCAD in diaphragms of WT and C3KO mice. Any protein that is an *in vivo* substrate for CAPN3 is expected to accumulate in protein extracts from C3KO muscles. As shown in Figure 5A, no difference was observed in the concentration of VLCAD between WT and C3KO mitochondrial extracts prepared from diaphragm muscles.

It was shown previously that a member of the calpain family, μ-calpain, is present in mitochondria, where it is involved in the regulation of mitochondrial proteins, including the regulation of apoptosis-inducing factor (29). To determine whether CAPN3 is also present in mitochondria, we performed western blot analysis of mitochondrial fractions isolated from diaphragms using anti-CAPN3 antibody. Figure 5B demonstrates that although CAPN3 is readily detectable in the cytosol- and membrane-containing WT supernatant, no CAPN3 was detected in mitochondrial fractions. Thus, despite the results of the proteomic analysis and *in vitro* cleavage experiments, we were not able to prove that VLCAD is a physiological substrate for CAPN3. Moreover, the absence of CAPN3 in mitochondrial extracts makes it unlikely that CAPN3 is directly involved in the regulation of any mitochondrial proteins, at least inside mitochondria.

Activity of VLCAD is decreased in C3KO muscles

Beta-oxidation of fatty acids occurs in close association with the inner membrane of mitochondria, and the integrity of

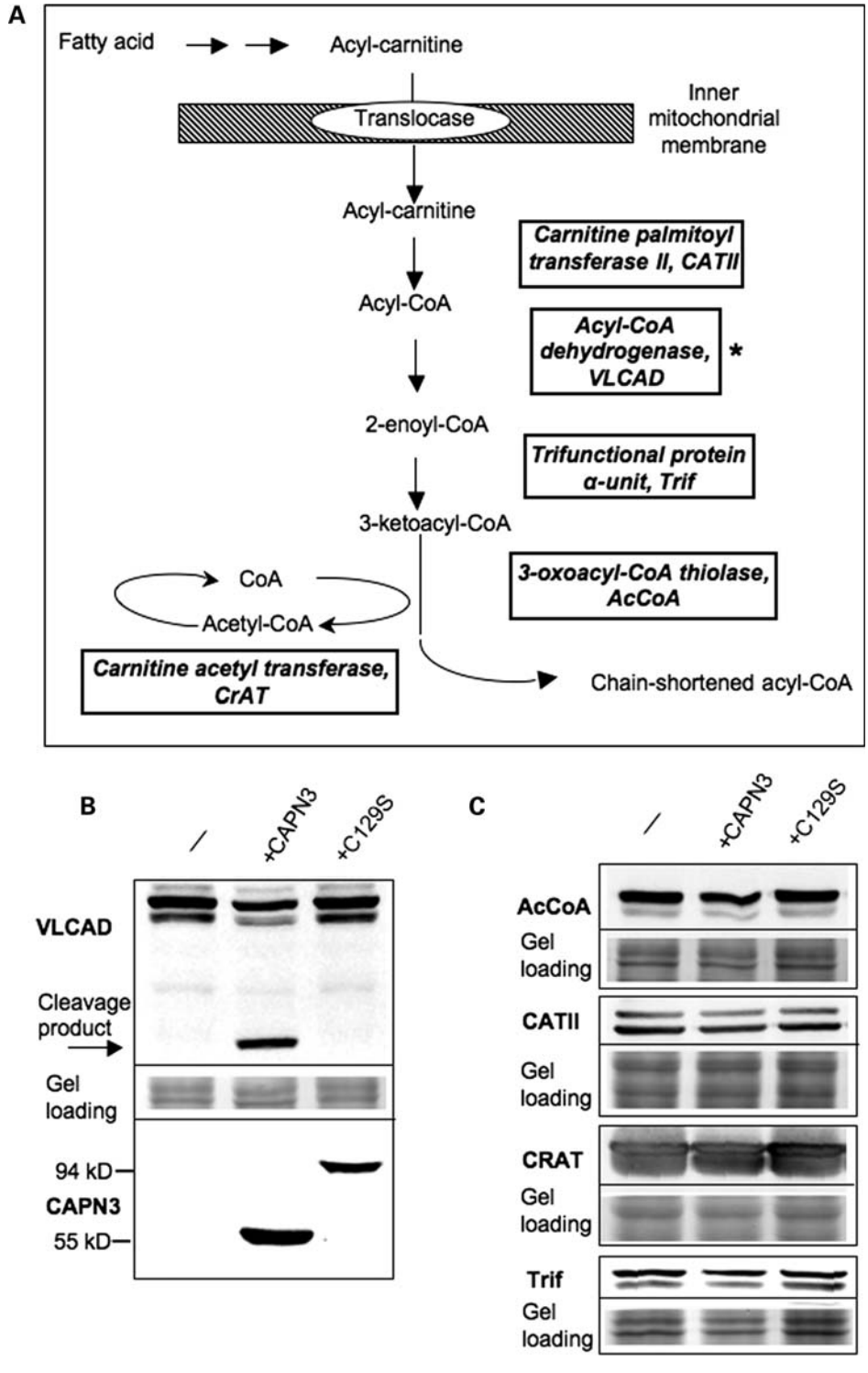

Figure 4. Assesment of mitochondrial proteins involved in β-oxidation of fatty acids as potential substrates for CAPN3 proteolytic activity. (**A**) Schematic of the β-oxidation pathway; only proteins that were identified in the proteomic screen (27) as putative substrates for CAPN3 are shown. (**B** and **C**) All potential substrates were cloned in baculoviral expression vectors with a V5 epitope tag introduced in frame at the C-terminal end of each protein. Each potential substrate was expressed alone (-) or co-expressed either with proteolytically active CAPN3 or the proteolytically inactive C129S mutant. If a protein can be cleaved by CAPN3, a decreased amount or additional cleavage product is expected upon co-expression with proteolytically active CAPN3. As shown in (B), VLCAD was the only protein cleaved by CAPN3; the arrow points to a product resulting from CAPN3 cleavage of VLCAD. Identical protein extracts were also stained for CAPN3 (B, bottom panel) to ensure its expression. Note that full-length CAPN3 undergoes almost complete autolysis and runs as a 55 kDa band (unlike the proteolytically inactive C129S mutant that runs as a 94 kDa band). Middle panel shows protein loading. (C) None of the other four proteins tested showed any change upon co-expression with active CAPN3 (since we did not detect any cleavage products, only full-length bands are shown).

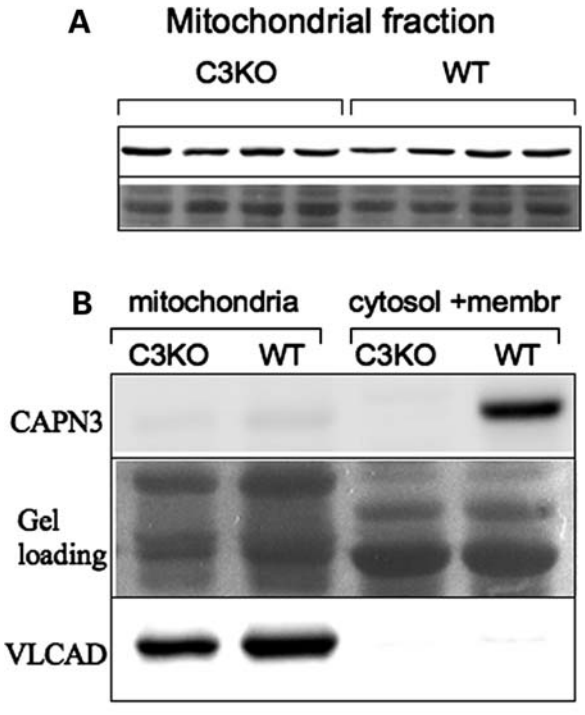

Figure 5. VLCAD concentration is not elevated in C3KO muscles. (**A**) Mitochondrial fractions from diaphragm muscles of four WT and four C3KO males were stained for VLCAD (upper panel). No difference was found between C3KO and WT muscles, suggesting that VLCAD is not a bone fide substrate of CAPN3 *in vivo*. (**B**) Although CAPN3 was readily detectable in the WT fraction that contained cytosol and membrane, no CAPN3 was detected in the mitochondrial fraction from WT muscle (upper panel). C3KO muscles were examined as a negative control. Staining with anti-VLCAD antibodies was performed to confirm that the mitochondrial fractionation was carried out successfully (lower panel). Middle panel shows protein loading.

this membrane has been suggested to be important for the pathway function. Mitochondrial membrane integrity was previously shown to be important for VLCAD activity. For example, during cardiac ischemia, the activity of VLCAD, but not its concentration, was decreased (30). As shown in Figure 1, mitochondria from C3KO muscles have a 'swollen' appearance, suggesting that the membrane integrity in those mitochondria may be disrupted. Even though the concentration of VLCAD was unchanged in C3KO mitochondria, we investigated whether the abnormal mitochondrial structure may be affecting VLCAD activity in C3KO muscles. These studies showed that VLCAD activity was decreased in C3KO diaphragm muscles by ~20% compared with WT (Fig. 6). Thus, even though CAPN3 does not regulate VLCAD directly, the activity of the enzyme is affected by the absence of CAPN3. Taken together, these results suggest that the absence of CAPN3 indirectly leads to reduced mitochondrial function.

Evidence of oxidative stress in C3KO muscles

Functionally deficient mitochondria are known to produce elevated reactive oxygen species (ROS) which leads to the oxidative modification of various macromolecules. This condition, called oxidative stress, has been shown to play an important role in the pathogenesis of many diseases such as cancer, neurodegeneration and cardiovascular disease, as well as in the normal physiological process of aging (31–34). To address the question of whether mitochondrial abnormalities might lead to oxidative stress in C3KO muscles, we used a protein oxidation detection kit (Chemicon) which allows for the detection of carbonyl groups introduced into protein side chains as a consequence of oxidative modification of proteins. As shown in Figure 7A, the level of oxidized proteins in C3KO diaphragm muscle extracts from 10–11-month-old animals was elevated compared with age-matched WT muscles. Interestingly, the accumulation of carbonyl-modified proteins appears to be progressive with age since the accumulation of oxidized proteins was much lower in C3KO mice at 2 months of age (Fig. 7B).

There are several mechanisms to protect cells against ROS, including enzymatic modification of the ROS. Antioxidant metalloenzymes, called superoxide dismutases (SOD), catalyze the redox dismutation of superoxide radical into the less harmful oxygen and hydrogen peroxide. An increased concentration of these enzymes is considered to be indicative of oxidative stress as a mechanism used by cells to buffer the extra ROS. Western blot analysis of Mn-SOD in extracts from 1-year-old C3KO and WT muscles is presented in Figure 7C. Quantitative analysis of this blot revealed an ~50% increase in the Mn-SOD concentration in C3KO muscles compared with WT muscles.

In conclusion, these data indicate that CAPN3 deficiency is associated with mitochondrial abnormalities and oxidative stress, and therapeutic management of these defects may be helpful for calpainopathy patients. Thus, these studies may reveal a novel therapeutic target for the treatment of LGMD2A.

DISCUSSION

In these studies, we described abnormalities in mitochondrial ultrastructure, distribution and function in skeletal muscles lacking the non-lysosomal cysteine protease CAPN3. We showed that these abnormalities likely represent a secondary effect of calpainopathy since CAPN3 is neither present in muscle mitochondrial fractions, nor can it cleave any of the mitochondrial proteins that we tested as potential CAPN3 substrates *in vivo*.

Mitochondrial abnormalities have been reported for several different types of muscular dystrophy, even those not caused by mutations in mitochondrial DNA or in genes coding for mitochondrial proteins. The most relevant to our study are the observations of increased and disorganized mitochondria in Japanese LGMD2A patients (12,13) and a clinical case of an LGMD2A patient with symptoms of a metabolic disorder (35). Decreased energy production and mitochondrial swelling were also reported for Duchenne muscular dystrophy caused by mutations in the dystrophin gene, in mice lacking δ-sarcoglycan or laminin α-2 chain, and in both the mouse model and patients with collagen VI myopathies (36–38). In all these cases, the mutated genes did not have a direct or obvious involvement in mitochondrial metabolism. Thus,

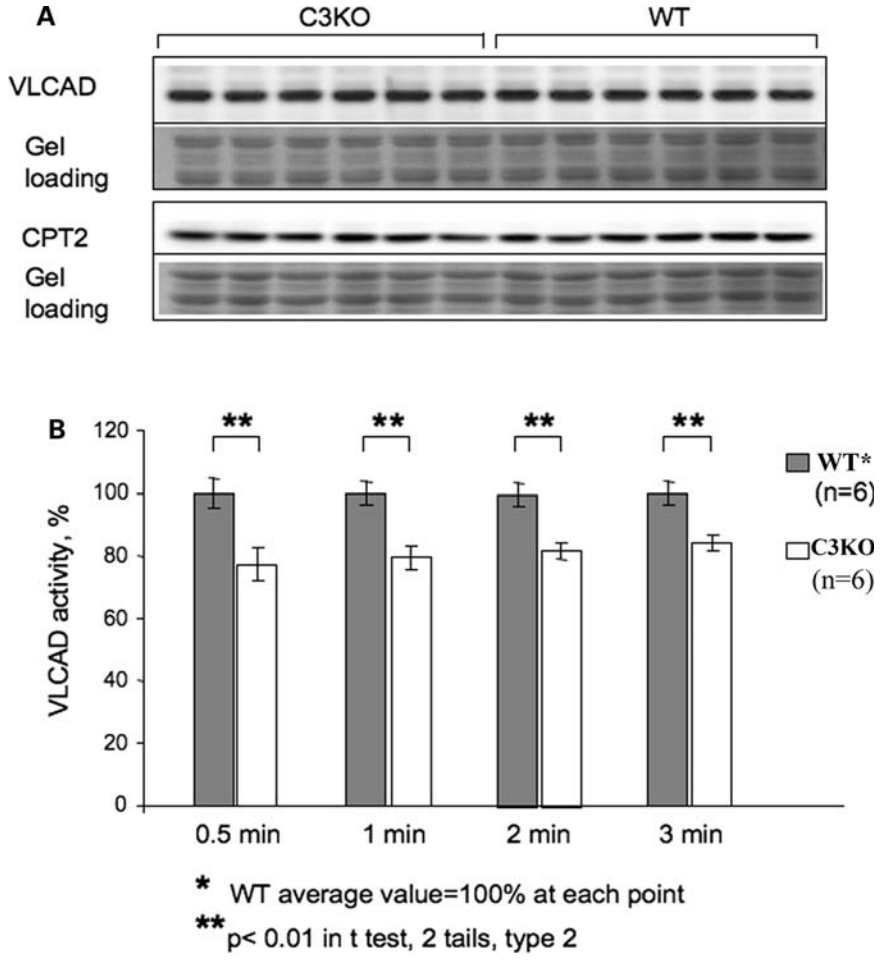

Figure 6. VLCAD activity is decreased in C3KO muscle. Mitochondria were isolated from six C3KO and six WT muscles for the analysis of VLCAD concentration and activity. (**A**) Western blots of mitochondrial fractions were stained with anti-VLCAD antibodies and with antibody against another mitochondrial protein (anti-CPT-2 antibody). (**B**) VLCAD activity assay. Protein concentration in the extracts was measured using the Bio-Rad Protein Assay Kit to ensure that an equal amount of the mitochondrial protein was used for measurements of VLCAD enzymatic activity. VLCAD activity was measured as described in Materials and Methods. Measurements of absorbance at 300 nm were taken after 30 s, 1 min and then every minute. The average WT VLCAD activity at each time point was set to be 100% activity. An ~20% decrease in VLCAD activity was found in C3KO muscles compared with WT.

mitochondrial abnormalities are likely a secondary feature of many different types of muscular dystrophy.

It is not clear why and how deficits in structural components of the dystroglycan complex (dystrophin, δ-sarcoglycan) or extracellular matrix proteins (collagen VI, laminin α-2 chain) may result in mitochondrial dysfunction. A leading hypothesis is that the impairment of the ability of the dystroglycan complex to interact with extracellular matrix proteins causes the instability of the sarcolemma and the influx of extracellular calcium. This, in turn, leads to increased intracellular calcium that is buffered by the mitochondria, which triggers changes in mitochondrial membrane permeability. Indeed, increased influx through a dystrophin-deficient membrane has been demonstrated; however, normal or even lower cytosolic calcium can be maintained in mdx muscles, possibly due to robust calcium homeostasis mechanisms (reviewed in 39). On the other hand, detailed studies of collagen VI-deficient myofibers that have abnormally swollen and dysfunctional mitochondria revealed no change in intracellular calcium levels even in the presence of 20 mM extracellular calcium (36). We did not find any evidence of sarcolemmal instability in C3KO mice. Even after treadmill running exercise or increased muscle loading, C3KO muscles did not show an increase in muscle membrane damage (18). Moreover, calcium release upon activation is decreased in C3KO muscle compared with WT (23). These data suggest that mechanisms other than calcium overload can trigger mitochondrial defects. One explanation for the mitochondrial abnormalities in calpainopathy might be decreased protein turnover of CAPN3 substrates in C3KO muscles. The accumulation of these proteins can lead to the formation of insoluble protein aggregates and increased cytotoxicity, which with time (in older animals) may affect normal mitochondrial homeostasis. We have some experimental support for the formation of insoluble aggregates in older C3KO mice, which was published earlier (18). Recently, it was shown that increased cytotoxicity induced by overexpression of Huntingtin proteins caused significant alterations in mitochondrial dynamics, particularly mitochondrial fragmentation (40).

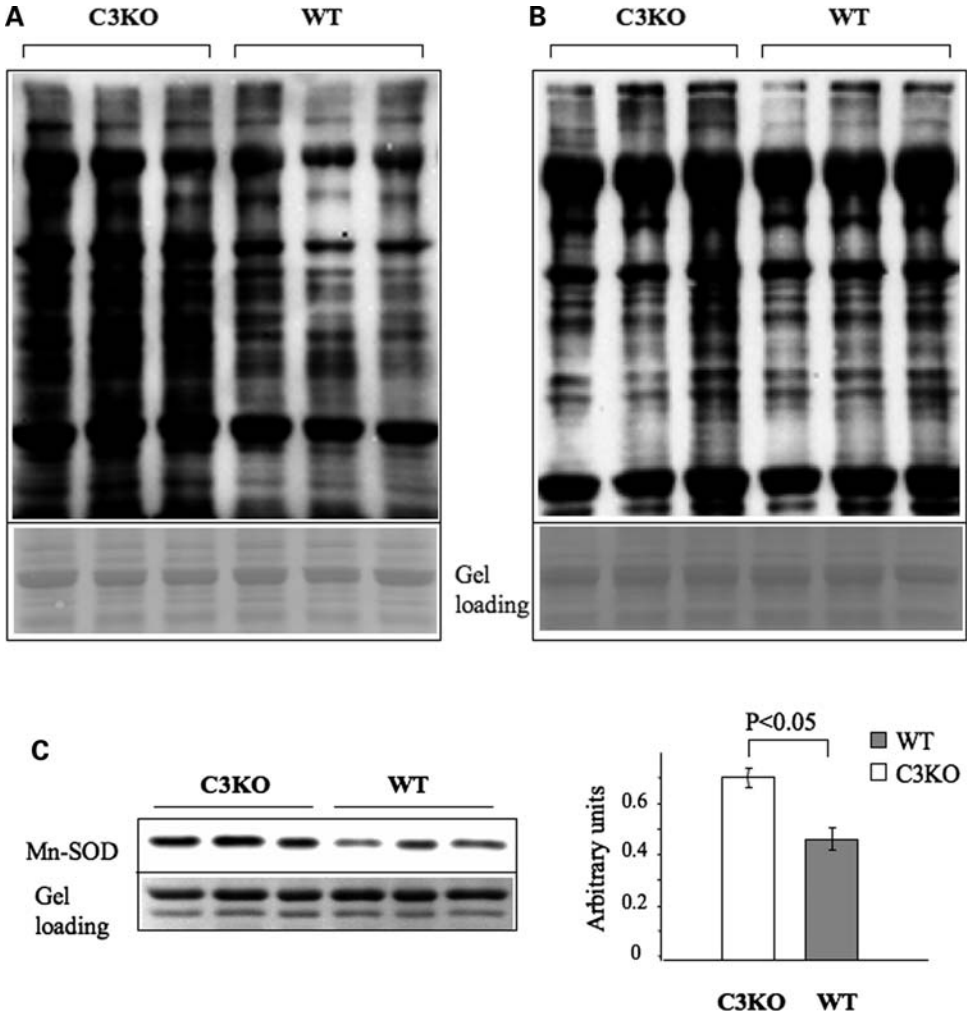

Figure 7. Evidence of increased oxidative stress in 1-year-old C3KO muscles. OxyBlot™ Protein Oxidation Detection Kit (Chemicon) was used for the immunoblot detection of carbonyl groups introduced into proteins by oxidative reactions. (**A**) Measurements of protein oxidation by OxyBlot in old C3KO mice. The concentration of oxidized proteins was higher in diaphragm muscles isolated from 10–11-month-old C3KO mice compared with diaphragm muscles isolated from WT mice of the same age. (**B**) Measurements of protein oxidation by OxyBlot in young C3KO mice. Only one out of three diaphragm extracts isolated from 2-month-old C3KO mice had an elevated concentration of oxidized proteins compared with the age-matched WT mice. (**C**) Quantitative western blot analysis showed that Mn-SOD concentration is also elevated in C3KO muscles from 1-year-old mice.

Even though the exact mechanisms that lead to mitochondrial abnormalities remain unclear, the overall harmful effects of this dysfunction on disease progression raise no doubts. Mitochondria are key regulators of cell survival, and the involvement of mitochondria in the pathogenesis of many progressive diseases has been observed in neurodegenerative diseases such as Alzheimer's disease, Parkinson's disease and amyotropic lateral sclerosis (41). Muscular dystrophies are also progressive disorders that lead to muscle cell death through necrotic or apoptotic mechanisms. Apoptosis, in particular, was shown to be elevated in LGMD2A patients (21). We did not find any evidence of increased apoptosis in C3KO mice (15) but the mice have a much milder disease phenotype compared with the LGMD2A patients. Since other signs of mitochondrial dysfunction are present in C3KO mice (such as a deficit of ATP production and increased oxidative stress), managing mitochondrial dysfunction by therapeutic means may provide benefits for patients with LGMD2A.

A few studies have been done that generated promising results in improving pathology through pharmacological correction of mitochondrial dysfunction (38,42). The loss of membrane potential and increased mitochondrial membrane permeability occurs owing to the opening of the so-called permeability transition pore (PTP). The PTP is a large protein complex that spans the outer and inner membranes, and its activation induces loss of potential and mitochondrial swelling (43). Recent studies in several diseases demonstrated that the PTP is a valid target for therapeutic management. First, it was shown that the treatment of collagen VI knockout mice with cyclosporin A (CsA), a widely used immunosuppressant that desensitizes the PTP and inhibits its opening, significantly decreased the number of apoptotic nuclei and improved overall muscle morphology (36). Myoblasts from human collagen VI-deficient myoblasts also showed improvement in mitochondrial morphology and apoptosis after treatment with CsA (42). Recently, CsA was used to treat four patients

with Ullrich congenital muscular dystrophy and one patient with Bethlem myopathy; both diseases are due to mutations in collagen VI (44). A significant improvement of mitochondrial dysfunction and apoptosis was found after 1 month of oral CsA administration.

More recently, another cyclosporine (Debio-025) that retains the PTP-desensitizing activity but does not interact with calcineurin and does not have an immunosuppressant effect became available (45). Debio-025 acts as an inhibitor of cyclophilin D, a mitochondrial matrix prolyl *cis–trans* isomerase that directly regulates mitochondrial permeability transition (46). Recently, double-knockout mice were described that carry deletions of either δ-sarcoglycan (one of the components of the dystroglycan protein complex) or laminin α-2 chain in combination with the deletion of cyclophilin D gene (38). Both types of the double-knockout mice showed markedly decreased dystrophic features in skeletal muscles and heart. Moreover, pharmacological inhibition of cyclophilin D with Debio-025 also reduced disease manifestation in δ-sarcoglycan-deficient and dystrophin-deficient mice (38,47). Debio-025 also improved phenotype of human collagen VI-deficient myoblasts and can potentially be used to treat mitochondrial dysfunction in patients (42).

Our studies demonstrate for the first time that mitochondrial abnormalities and associated energy production deficits along with increased oxidative stress are pathogenic features of calpainopathy. Pharmacological correction of mitochondrial abnormalities, common for different types of muscular dystrophies, is emerging as a new therapeutic avenue for improving the quality of life for muscular dystrophy patients. These studies in the C3KO mouse suggest that pharmacological control of these conditions could also be beneficial for LGMD2A patients.

MATERIALS AND METHODS

Electron microscopy and histochemistry

Diaphragm and soleus muscles were prepared for electron microscopy as described previously (48). Briefly, muscles were dissected from three WT and three C3KO mice and fixed in 1.4% glutaraldehyde in 0.2 M sodium cacodylate buffer, pH 7.2 for 30 min on ice, followed by buffer rinse and fixation for 30 min in 1% osmium tetroxide. Sections were prepared from the epoxy resin embedded samples and examined under the electron microscope model JEM-1200EX (JEOL, Japan) equipped with BioScan 600 W digital camera (1024 × 1024 pixels). DigitalMicrograph 1.2 software (Gatan, USA) was used to generate images.

NADH and SDH staining was performed on 8 μm transverse cryostat sections after quenching in liquid nitrogen as described previously (49).

In vivo mitochondrial ATP production

^{31}P MRS measurements were performed on the hind limb muscles of seven WT and eight CAPN3 knockout mice (all 6–7-month-old). All spectra were acquired using an 11.1 T/470 MHz Bruker spectrometer (PV3.02) and a custom-built 6 mm × 12 mm oblong ^{31}P surface coil. The mice were anesthetized using 1.5% gaseous isoflurane. The animal's right hind limb was extended, and the ^{31}P surface coil was placed over the belly of the gastrocnemius muscle. A 3 cm ^{1}H surface coil was placed underneath the hind limb to perform localized shimming. An inflatable blood pressure cuff was positioned around the animal's thigh.

A reversible ischemia model was used to study kinetic changes in the energy-rich Pi content and the rate of PCr recovery, a measure of *in vivo* mitochondrial function. A 30 min period of ischemia was chosen to induce ∼50% depletion in the PCr content and a minimal change in pHi, as described previously (50,51). Spectra were acquired with a 50 μs square pulse, a pulse repetition time of 2 s, sweep width of 10 000 Hz and 8000 complex data points. Sequential ^{31}P spectra were acquired in 30 s bins at rest (10 min), during ischemia (30 min) and throughout recovery (30 min).

The spectra were manually phased and the areas of the γ-ATP, inorganic Pi and PCr peaks at rest were determined using area integration and corrected for saturation (50,51). Kinetic changes in PCr during recovery were measured using principal component analysis (52). The initial rate of PCr recovery (mM min^{-1}), a direct measure of ATP synthesis, was determined during the first 3 min following the restoration of blood flow. pHi was calculated from the chemical shift of Pi.

Tissue processing and citrate synthase activity assay

Frozen tibialis anterior or diaphragm was thawed in iced 0.15 M KCl solution, blotted, weighed and transferred to a hand-held glass Potter homogenizer in 10 vol:weight homogenization buffer (20 mM HEPES, 120 mM KCl, 5 mM $MgCl_2$, 1 mM EGTA, pH 7.2, 0.5% fatty acid free BSA, 50 U/ml sodium heparin). The 10% homogenate was centrifuged at 1000*g* for 20 min. The supernatant was frozen and thawed four times and then diluted 1:10 vol:vol in 50 mM potassium phosphate, 250 mM sucrose, 0.5% taurodeoxycholic acid, pH 7.0, in order to break open the mitochondrial membranes and release citrate synthase. The diluted sample was kept on ice. Citrate synthase activity was assayed by following the release of CoA-SH at 25°C by increasing absorbance at 412 nm owing to the reaction of CoA-SH with 5,5′-dithiobis-2-nitro-benzoic acid (DTNB, Ellman's reagent) to yield 5-thio-2-nitro-benzoic acid (TNB). Reaction mix consisted of 0.1 mM DTNB, 0.3 mM acetyl-CoA, 0.5 mM oxaloacetate and the diluted supernatant. An extinction coefficient of 13.6 mM^{-1} cm^{-1} was used to calculate the rate of TNB formation and citrate synthase activity.

Muscle protein extract preparation for western blot analysis and protein oxidation detection

For western blot analysis, diaphragm muscles were homogenized in a Dounce homogenizer in reducing sample buffer [80 mM Tris, pH 6.8, 0.1 M dithiothreitol, 2% SDS and 10% glycerol with protease inhibitors cocktail (Sigma)]. The following antibodies were used in this study: mouse anti-CAPN3 12A2 antibody (Novocastra), mouse anti-V5 (Invitrogen), mouse anti-Mn-SOD (BD Transduction Labs). The antibody against VLCAD was a generous gift from Dr Arnold W. Strauss (Vanderbilt Children's Hospital, Nashville, TN, USA).

OxyBlot™ Protein Oxidation Detection Kit (Chemicon) was used for immunoblot detection of carbonyl groups introduced

into proteins by oxidative reactions, according to the manufacturer's instructions. SDS-containing sample buffer with reduced DTT concentration (80 mM Tris, pH 6.8, 50 mM dithiothreitol, 2% SDS and 10% glycerol) was used for muscle protein extraction; 20 μg of total muscle protein was used for each derivatization reaction. A total of six C3KO and six WT diaphragm muscles were analyzed in these experiments.

Cloning of mitochondrial proteins cDNAs and protein co-expression

Full-length cDNAs for mitochondrial proteins identified in the previously performed proteomic screen were produced using RT–PCR. Primers were chosen on the basis of the following Genbank sequences: acyl-coenzyme A dehydrogenase, very long chain (VLCAD), BC026559; carnitine *O*-palmitoyl transferase II (CATII), U01163; acetyl-coenzyme A acyltransferase (AcCoA), BC028901; trifunctional protein alpha subunit (Trif), AK029017; carnitine acetyltransferase (CrAT), X85983.

To test whether CAPN3 could cleave any of the mitochondrial proteins identified by proteomic comparison (27), WT CAPN3 or the inactive C129S mutant was cloned into pVL1393 baculoviral transfer vector without any tags to ensure proper protease activity. Individual mitochondrial proteins tagged with V5 epitope peptide, and CAPN3 constructs were co-expressed in a baculovirus system (BD Biosciences) according to the manufacturer's instruction. Insect cells were plated on 10 cm cell culture dishes at 50–70% of confluence and co-infected with plasmids coding for the mitochondrial protein and CAPN3 high-titer viral stocks. After incubation for 3 days at 27°C, cells were harvested by lysis in Insect Cell Lysis Buffer (BD Biosciences) with Protease Inhibitor Cocktail (Sigma, 1:100). Soluble fractions were analyzed by western blotting using anti-V5 (Invitrogen) or anti-CAPN3 antibody 12A2 (Novocastra) to detect mitochondrial proteins or CAPN3, respectively.

Isolation of mitochondria and measurement of VLCAD activity

To isolate mitochondria, diaphragm muscles were homogenized in 15 volumes of buffer containing 0.25 M sucrose, 0.2 mM EDTA and 10 mM Tris–HCl, pH 7.8. Homogenates were centrifuged for 8 min at 2000*g* at 4°C, and resulting supernatants were centrifuged for 15 min at 12 000*g* at 4°C. Pellets that contained mitochondria were washed several times with the same buffer. For the measurement of VLCAD activity, mitochondria were either sonicated on ice with three pulses of 3 s each or treated with Triton X-100 at a final concentration of 0.01% (30).

Assay of VLCAD activity was performed as described previously (30,53). Briefly, 20 μg of mitochondrial protein was used for each reaction that was performed in buffer containing 20 mM MOPS, 0.5 mM EDTA and 200 μM of ferrocenium hexafluorophosphate (Sigma Aldrich). Palmitoyl-CoA was used as a substrate at 100 μM concentration. The reduction of ferrocenium hexafluorophosphate to the neutral ferrocene derivative by the active VLCAD upon substrate addition results in decreased absorbance at 300 nm. Measurements were taken after 30 s, 1 min and then every minute for the next 3 min.

FUNDING

This work was supported by grants to M.J.S. awarded by the National Institute of Health (NIAMS, RO1, AR 48177) and the Muscular Dystrophy Association.

ACKNOWLEDGEMENTS

NMR data were obtained at the Advanced Magnetic Resonance Imaging and Spectroscopy Facility in the McKnight Brain Institute of the University of Florida with the support of the National High Magnetic Field Laboratory.

Conflict of Interest statement. None declared.

REFERENCES

1. Goll, D.E., Thompson, V.F., Li, H., Wei, W. and Cong, J. (2003) The calpain system. *Physiol. Rev.*, **83**, 731–801.
2. Suzuki, K., Hata, S., Kawabata, Y. and Sorimachi, H. (2004) Structure, activation, and biology of calpain. *Diabetes*, **53** (Suppl. 1), S12–S18.
3. Richard, I., Broux, O., Allamand, V., Fougerousse, F., Chiannilkulchai, N., Bourg, N., Brenguier, L., Devaud, C., Pasturaud, P., Roudaut, C. *et al.* (1995) Mutations in the proteolytic enzyme calpain 3 cause limb-girdle muscular dystrophy type 2A. *Cell*, **81**, 27–40.
4. Groen, E.J., Charlton, R., Barresi, R., Anderson, L.V., Eagle, M., Hudson, J., Koref, M.S., Straub, V. and Bushby, K.M. (2007) Analysis of the UK diagnostic strategy for limb girdle muscular dystrophy 2A. *Brain*, **130**, 3237–3249.
5. Kramerova, I., Beckmann, J.S. and Spencer, M.J. (2007) Molecular and cellular basis of calpainopathy (limb girdle muscular dystrophy type 2A). *Biochim. Biophys. Acta*, **1772**, 128–144.
6. Laval, S.H. and Bushby, K.M. (2004) Limb-girdle muscular dystrophies—from genetics to molecular pathology. *Neuropathol. Appl. Neurobiol.*, **30**, 91–105.
7. Milic, A., Daniele, N., Lochmuller, H., Mora, M., Comi, G.P., Moggio, M., Noulet, F., Walter, M.C., Morandi, L., Poupiot, J. *et al.* (2007) A third of LGMD2A biopsies have normal calpain 3 proteolytic activity as determined by an in vitro assay. *Neuromuscul. Disord.*, **17**, 148–156.
8. Fanin, M., Nascimbeni, A.C., Fulizio, L. and Angelini, C. (2005) The frequency of limb girdle muscular dystrophy 2A in northeastern Italy. *Neuromuscul. Disord.*, **15**, 218–224.
9. Saenz, A., Leturcq, F., Cobo, A.M., Poza, J.J., Ferrer, X., Otaegui, D., Camano, P., Urtasun, M., Vilchez, J., Gutierrez-Rivas, E. *et al.* (2005) LGMD2A: genotype–phenotype correlations based on a large mutational survey on the calpain 3 gene. *Brain*, **128**, 732–742.
10. Fardeau, M., Eymard, B., Mignard, C., Tomé, F.M., Richard, I. and Beckmann, J.S. (1996) Chromosome 15-linked limb-girdle muscular dystrophy: clinical phenotypes in Reunion Island and French metropolitan communities. *Neuromuscul. Disord.*, **6**, 447–453.
11. Urtasun, M., Saenz, A., Roudaut, C., Poza, J.J., Urtizberea, J.A., Cobo, A.M., Richard, I., Garcia Bragado, F., Leturcq, F., Kaplan, J.C. *et al.* (1998) Limb-girdle muscular dystrophy in Guipuzcoa (Basque Country, Spain). *Brain*, **121**, 1735–1747.
12. Kawai, H., Akaike, M., Kunishige, M., Inui, T., Adachi, K., Kimura, C., Kawajiri, M., Nishida, Y., Endo, I., Kashiwagi, S. *et al.* (1998) Clinical, pathological, and genetic features of limb-girdle muscular dystrophy type 2A with new calpain 3 gene mutations in seven patients from three Japanese families. *Muscle Nerve*, **21**, 1493–1501.
13. Chae, J., Minami, N., Jin, Y., Nakagawa, M., Murayama, K., Igarashi, F. and Nonaka, I. (2001) Calpain 3 gene mutations: genetic and clinico-pathologic findings in limb-girdle muscular dystrophy. *Neuromuscul. Disord.*, **11**, 547–555.
14. Hermanova, M., Zapletalova, E., Sedlackova, J., Chrobakova, T., Letocha, O., Kroupova, I., Zamecnik, J., Vondracek, P., Mazanec, R., Marikova, T.

et al. (2006) Analysis of histopathologic and molecular pathologic findings in Czech LGMD2A patients. *Muscle Nerve*, **33**, 424–432.
15. Kramerova, I., Kudryashova, E., Tidball, J.G. and Spencer, M.J. (2004) Null mutation of calpain 3 (p94) in mice causes abnormal sarcomere formation in vivo and in vitro. *Hum. Mol. Genet.*, **13**, 1373–1388.
16. Richard, I., Roudaut, C., Marchand, S., Baghdiguian, S., Herasse, M., Stockholm, D., Ono, Y., Suel, L., Bourg, N., Sorimachi, H. *et al.* (2000) Loss of calpain 3 proteolytic activity leads to muscular dystrophy and to apoptosis-associated IKBa/nuclear factor KB pathway perturbation in mice. *J. Cell Biol.*, **151**, 1–9.
17. Spencer, M.J., Guyon, J.R., Sorimachi, H., Potts, A., Richard, I., Herasse, M., Chamberlain, J., Dalkilic, I., Kunkel, L.M. and Beckmann, J.S. (2002) Stable expression of calpain 3 from a muscle transgene in vivo: immature muscle in transgenic mice suggests a role for calpain 3 in muscle maturation. *Proc. Natl Acad. Sci. USA*, **99**, 8874–8879.
18. Kramerova, I., Kudryashova, E., Venkatraman, G. and Spencer, M.J. (2005) Calpain 3 participates in sarcomere remodeling by acting upstream of the ubiquitin–proteasome pathway. *Hum. Mol. Genet.*, **14**, 2125–2134.
19. Kramerova, I., Kudryashova, E., Wu, B. and Spencer, M.J. (2006) Regulation of the M-cadherin-beta-catenin complex by calpain 3 during terminal stages of myogenic differentiation. *Mol. Cell. Biol.*, **26**, 8437–8447.
20. Taveau, M., Bourg, N., Sillon, G., Roudaut, C., Bartoli, M. and Richard, I. (2003) Calpain 3 is activated through autolysis within the active site and lyses sarcomeric and sarcolemmal components. *Mol. Cell. Biol.*, **23**, 9127–9135.
21. Baghdiguian, S., Martin, M., Richard, I., Pons, F., Astier, C., Bourg, N., Hay, R.T., Chemaly, R., Halaby, G., Loiselet, J. *et al.* (1999) Calpain 3 deficiency is associated with myonuclear apoptosis and profound perturbation of the IkappaB alpha/NF-kappaB pathway in limb-girdle muscular dystrophy type 2A. *Nat. Med.*, **5**, 503–511 [Published erratum appeared in *Nat. Med.*, **5,** 849 (1999)].
22. Benayoun, B., Baghdiguian, S., Lajmanovich, A., Bartoli, M., Daniele, N., Gicquel, E., Bourg, N., Raynaud, F., Pasquier, M.A., Suel, L. *et al.* (2008) NF-kappaB-dependent expression of the antiapoptotic factor c-FLIP is regulated by calpain 3, the protein involved in limb-girdle muscular dystrophy type 2A. *FASEB J.*, **22**, 1521–1529.
23. Kramerova, I., Kudryashova, E., Wu, B., Ottenheijm, C., Granzier, H. and Spencer, M.J. (2008) Novel role of calpain-3 in the triad-associated protein complex regulating calcium release in skeletal muscle. *Hum. Mol. Genet.*, **17**, 3271–3280.
24. Sorimachi, H., Kinbara, K., Kimura, S., Takahashi, M., Ishiura, S., Sasagawa, N., Sorimachi, N., Shimada, H., Tagawa, K., Maruyama, K. *et al.* (1995) Muscle-specific calpain, p94, responsible for limb girdle muscular dystrophy type 2A, associates with connectin through IS2, a p94-specific sequence. *J. Biol. Chem.*, **270**, 31158–31162.
25. Kinbara, K., Sorimachi, H., Ishiura, S. and Suzuki, K. (1997) Muscle-specific calpain, p94, interacts with the extreme C-terminal region of connectin, a unique region flanked by two immunoglobulin C2 motifs. *Arch. Biochem. Biophys.*, **342**, 99–107.
26. Huang, Y., de Morree, A., van Remoortere, A., Bushby, K., Frants, R.R., Dunnen, J.T. and van der Maarel, S.M. (2008) Calpain 3 is a modulator of the dysferlin protein complex in skeletal muscle. *Hum. Mol. Genet.*, **17**, 1855–1866.
27. Cohen, N., Kudryashova, E., Kramerova, I., Anderson, L.V., Beckmann, J.S., Bushby, K. and Spencer, M.J. (2006) Identification of putative in vivo substrates of calpain 3 by comparative proteomics of overexpressing transgenic and nontransgenic mice. *Proteomics*, **6**, 6075–6084.
28. DiMauro, S. and Schon, E.A. (2003) Mitochondrial respiratory-chain diseases. *N. Engl. J. Med.*, **348**, 2656–2668.
29. Garcia, M., Bondada, V. and Geddes, J.W. (2005) Mitochondrial localization of mu-calpain. *Biochem. Biophys. Res. Commun.*, **338**, 1241–1247.
30. Mason, K.E., Stofan, D.A. and Szweda, L.I. (2005) Inhibition of very long chain acyl-CoA dehydrogenase during cardiac ischemia. *Arch. Biochem. Biophys.*, **437**, 138–143.
31. Lubos, E., Handy, D.E. and Loscalzo, J. (2008) Role of oxidative stress and nitric oxide in atherothrombosis. *Front. Biosci.*, **13**, 5323–5344.
32. Zeevalk, G.D., Bernard, L.P., Song, C., Gluck, M. and Ehrhart, J. (2005) Mitochondrial inhibition and oxidative stress: reciprocating players in neurodegeneration. *Antioxid. Redox Signal.*, **7**, 1117–1139.
33. Moore, D.J., West, A.B., Dawson, V.L. and Dawson, T.M. (2005) Molecular pathophysiology of Parkinson's disease. *Annu. Rev. Neurosci.*, **28**, 57–87.
34. Ungvari, Z., Buffenstein, R., Austad, S.N., Podlutsky, A., Kaley, G. and Csiszar, A. (2008) Oxidative stress in vascular senescence: lessons from successfully aging species. *Front. Biosci.*, **13**, 5056–5070.
35. Pénisson-Besnier, I., Richard, I., Dubas, F., Beckmann, J.S. and Fardeau, M. (1998) Pseudometabolic expression and phenotypic variability of calpain deficiency in two siblings. *Muscle Nerve*, **21**, 1078–1080.
36. Irwin, W.A., Bergamin, N., Sabatelli, P., Reggiani, C., Megighian, A., Merlini, L., Braghetta, P., Columbaro, M., Volpin, D., Bressan, G.M. *et al.* (2003) Mitochondrial dysfunction and apoptosis in myopathic mice with collagen VI deficiency. *Nat. Genet.*, **35**, 367–371.
37. Kuznetsov, A.V., Winkler, K., Wiedemann, F.R., von Bossanyi, P., Dietzmann, K. and Kunz, W.S. (1998) Impaired mitochondrial oxidative phosphorylation in skeletal muscle of the dystrophin-deficient mdx mouse. *Mol. Cell. Biochem.*, **183**, 87–96.
38. Millay, D.P., Sargent, M.A., Osinska, H., Baines, C.P., Barton, E.R., Vuagniaux, G., Sweeney, H.L., Robbins, J. and Molkentin, J.D. (2008) Genetic and pharmacologic inhibition of mitochondrial-dependent necrosis attenuates muscular dystrophy. *Nat. Med.*, **14**, 442–447.
39. Deconinck, N. and Dan, B. (2007) Pathophysiology of Duchenne muscular dystrophy: current hypotheses. *Pediatr. Neurol.*, **36**, 1–7.
40. Wang, H., Lim, P.J., Karbowski, M. and Monteiro, M.J. (2009) Effects of overexpression of huntingtin proteins on mitochondrial integrity. *Hum. Mol. Genet.*, **18**, 737–752.
41. Lin, M.T. and Beal, M.F. (2006) Mitochondrial dysfunction and oxidative stress in neurodegenerative diseases. *Nature*, **443**, 787–795.
42. Angelin, A., Tiepolo, T., Sabatelli, P., Grumati, P., Bergamin, N., Golfieri, C., Mattioli, E., Gualandi, F., Ferlini, A., Merlini, L. *et al.* (2007) Mitochondrial dysfunction in the pathogenesis of Ullrich congenital muscular dystrophy and prospective therapy with cyclosporins. *Proc. Natl Acad. Sci. USA*, **104**, 991–996.
43. Rasola, A. and Bernardi, P. (2007) The mitochondrial permeability transition pore and its involvement in cell death and in disease pathogenesis. *Apoptosis*, **12**, 815–833.
44. Merlini, L., Angelin, A., Tiepolo, T., Braghetta, P., Sabatelli, P., Zamparelli, A., Ferlini, A., Maraldi, N.M., Bonaldo, P. and Bernardi, P. (2008) Cyclosporin A corrects mitochondrial dysfunction and muscle apoptosis in patients with collagen VI myopathies. *Proc. Natl Acad. Sci. USA*, **105**, 5225–5229.
45. Hansson, M.J., Mattiasson, G., Mansson, R., Karlsson, J., Keep, M.F., Waldmeier, P., Ruegg, U.T., Dumont, J.M., Besseghir, K. and Elmer, E. (2004) The nonimmunosuppressive cyclosporin analogs NIM811 and UNIL025 display nanomolar potencies on permeability transition in brain-derived mitochondria. *J. Bioenerg. Biomembr.*, **36**, 407–413.
46. Baines, C.P., Kaiser, R.A., Purcell, N.H., Blair, N.S., Osinska, H., Hambleton, M.A., Brunskill, E.W., Sayen, M.R., Gottlieb, R.A., Dorn, G.W. *et al.* (2005) Loss of cyclophilin D reveals a critical role for mitochondrial permeability transition in cell death. *Nature*, **434**, 658–662.
47. Reutenauer, J., Dorchies, O.M., Patthey-Vuadens, O., Vuagniaux, G. and Ruegg, U.T. (2008) Investigation of Debio 025, a cyclophilin inhibitor, in the dystrophic mdx mouse, a model for Duchenne muscular dystrophy. *Br. J. Pharmacol.*, **155**, 574–584.
48. Tidball, J.G., Albrecht, D.E., Lokensgard, B.E. and Spencer, M.J. (1995) Apoptosis precedes necrosis of dystrophin-deficient muscle. *J. Cell Sci.*, **108**, 2197–2204.
49. Verity, M.A. (1991) Infantile Pompe's disease, lipid storage, and partial carnitine deficiency. *Muscle Nerve*, **14**, 435–440.
50. Liu, M., Walter, G.A., Pathare, N.C., Forster, R.E. and Vandenborne, K. (2007) A quantitative study of bioenergetics in skeletal muscle lacking carbonic anhydrase III using 31P magnetic resonance spectroscopy. *Proc. Natl Acad. Sci. USA*, **104**, 371–376.
51. Pathare, N., Vandenborne, K., Liu, M., Stevens, J.E., Li, Y., Frimel, T.N. and Walter, G.A. (2008) Alterations in inorganic phosphate in mouse hindlimb muscles during limb disuse. *NMR Biomed.*, **21**, 101–110.
52. Elliott, M.A., Walter, G.A., Swift, A., Vandenborne, K., Schotland, J.C. and Leigh, J.S. (1999) Spectral quantitation by principal component analysis using complex singular value decomposition. *Magn. Reson. Med.*, **41**, 450–455.
53. Lehman, T.C., Hale, D.E., Bhala, A. and Thorpe, C. (1990) An acyl-coenzyme A dehydrogenase assay utilizing the ferricenium ion. *Anal. Biochem.*, **186**, 280–284.